https://doi.org/10.5194/egusphere-2026-1575
Preprint. Discussion started: 1 April 2026

Sea Salt Aerosols from Blowing Snow: Contributions to Radiative Forcing

Kalle Nordling[1], Joonas Merikanto[1], Petri Räisänen[1], Arundathi Chandrasekharan[1], and Risto Makkonen[1]

[1]Finnish Meteorological Institute, Helsinki, Finland

Correspondence: Kalle Nordling (kalle.nordling@fmi.fi)

Abstract. The Arctic and Antarctic regions experience significant climate impacts from aerosol-cloud-radiation interactions, yet the role of sea salt aerosols (SSA) emitted through blowing snow remains poorly quantified. This study implements a parameterization of the SSA production of blowing snow in both the TM5 global chemical transport model and the EC-Earth3 global climate model, for AMIP-type as well as transient (SSP3-7.0 for 2015-2051) experiments, assessing the contributions of the blowing snow process to aerosol mass, number, cloud condensation nuclei (CCN) and radiative forcing in both polar regions. Model results are evaluated against observations from the MOSAiC campaign and coastal stations (Villum, Zeppelin, Alert). EC-Earth3 Simulations show that blowing snow substantially increases SSA concentrations during polar winter and spring, especially in the Antarctic where enhancements can exceed 100% increase in particle numbers, leading to improved agreement with surface and in situ observations. Regionally, TM5 reveals an increase in accumulation mode aerosol and CCN. The resulting surface radiative forcing is globally negative due to increased scattering of shortwave radiation, while enhanced CCN increases longwave cloud effects in the polar lower troposphere. Overall, this work demonstrates that including blowing snow SSA emissions is essential for realistically representing polar aerosol burdens, seasonal cycles, and climate feedbacks in global models.

1 Introduction

The Arctic region is experiencing rapid climate change, warming nearly four times faster than the global average (Rantanen et al., 2022). This phenomenon, known as Arctic amplification, is driven by multiple feedback mechanisms, including changes in surface albedo, sea ice loss, and atmospheric heat transport (Serreze and Barry, 2011; Pithan and Mauritsen, 2014). Recently, the role of atmospheric aerosols has received increasing attention (Schmale et al., 2021). This is due to their complex interactions with atmospheric radiation, clouds, and surface albedo in the polar environments (Sand et al., 2017), and due to the effect of global aerosol emissions on the heat transport to the Arctic (Acosta Navarro et al., 2016; Lewinschal et al., 2019; Merikanto et al., 2021)). With regards to aerosol-cloud interactions in the polar regions, the longwave radiative effect

https://doi.org/10.5194/egusphere-2026-1575
Preprint. Discussion started: 1 April 2026

of low-level mixed-phase clouds, comprising both liquid droplets and ice crystals, plays a critical role (Mauritsen et al., 2011; Schmale et al., 2021). However, the overall impact of aerosols on Arctic clouds and climate is still not well understood. This is to a large extent because aerosol sources and their properties in the central Arctic are poorly known (Wendisch et al., 2019).

Sea salt aerosols (SSA) are an important source of cloud condensation nuclei (CCN) in the polar regions. Model estimates show that SSA account for more than a quarter of the Arctic aerosol number concentration. Their role is expected to become even more significant in a future climate with more open ocean and sea ice leads, leading to higher Arctic CCN concentrations (Emme and Horowitz, 2025). SSA represents the largest mass fraction among all aerosol species in the Arctic (May et al., 2016). The primary sources of SSA in the region are bubble bursting over open ocean and emissions from leads in sea ice(Lapere et al., 2024). However, recent studies have highlighted that blowing snow is also an important and previously underappreciated source of SSA, especially during winter and spring (Huang et al., 2018; Yang et al., 2008; Frey et al., 2020).

The first observations of SSA production from snow-covered sea ice were made in 2013 in the Weddell Sea, Antarctica. Frey et al. (2020) demonstrated that snow over sea ice can release sea salt into the atmosphere. Similar observations were made in the Arctic during the 2019–2020 MOSAiC expedition. Ranjithkumar et al. (2025) showed that both particle mass and number concentrations of SSA increased during periods of storm-induced blowing snow. Blowing snow was responsible for enhanced SSA concentrations for up to 40% of the time during the Arctic winter and spring.

CMIP6 models have been shown to inadequately represent SSA emissions in polar regions. In addition, there are significant discrepancies between models, largely due to differences in source functions and emission parameterizations (Lapere et al., 2023). These inconsistencies lead to biases in cloud microphysics, aerosol–radiation interactions, and the surface energy budget. Another source of model uncertainty is how SSA emissions are parameterized. Thornhill et al. (2021) demonstrated that doubling SSA emissions in CMIP6 models results in an effective radiative forcing ranging from $-0.3\ \mathrm{W\,m^{-2}}$ to $-2.2\ \mathrm{W\,m^{-2}}$. Furthermore, Venugopal et al. (2025) showed that this model spread is mainly due to differences in the parameterization of ambient aerosol size distribution, CCN, and cloud droplet number concentrations (CDNC).

The climate effects of SSA production from blowing snow remain uncertain. Gong et al. (2023) investigated this process using the GEOS-Chem chemical transport model, which was driven by meteorological fields from MERRA-2 reanalysis. Yang et al. (2019), Gong et al. (2023) and Ranjithkumar et al. (2025) implemented blowing snow SSA production in the p-TOMCAT chemical transport model. However, simulations using fully coupled global climate models are still lacking, limiting our understanding of the broader climate implications of SSA production from blowing snow.

Here, we implement SSA production from blowing snow into a chemical transport model TM5 and to a global climate model EC-Earth3 using TM5, based on the parameterization from Yang et al. (2019), to investigate the climate impacts of SSA from blowing snow and their effects on CCN and CDNC. We also investigate how much SSA is generated from blowing snow in the years 2019–2020 in both the Arctic and Antarctic using the TM5 chemical transport model, allowing for a direct comparison of the model results to Arctic in-situ MOSAiC campaign data as well as to data from monitoring stations at Zeppelin, Alert and Villum. Furthermore, we quantify the effective radiative forcing associated with blowing snow SSA using atmosphere-only (AMIP-style) simulations with the EC-Earth3 global climate model, and carry out transient climate simulations following the SSP3-7.0 scenario for the years 2015-2051 to investigate future responses to polar SSA changes.

https://doi.org/10.5194/egusphere-2026-1575
Preprint. Discussion started: 1 April 2026

2 Methods

2.1 Statistical methods

To assess the statistical significance of changes in aerosol particle number concentrations between simulations with and without blowing snow emissions, we applied a non-parametric block bootstrap method combined with False Discovery Rate (FDR) correction to control for multiple testing. At each grid point, we constructed a time series of monthly mean differences between the two simulations. To account for temporal autocorrelation, we applied the moving block bootstrap technique.

2.2 Observational datasets

Measurements of Arctic aerosols and cloud properties were carried out as part of the MOSAiC expedition. This year-long campaign, from September 2019 to October 2020, aimed to investigate Arctic climate change from multiple perspectives, including the atmosphere, sea ice, snow, ocean, ecosystems, and biogeochemistry (Shupe et al., 2020). Particle number concentration data from Beck et al. (2022) and cloud condensation nuclei (CCN) data from Bergner et al. (2023) were obtained for the MOSAiC expedition (October 2019–September 2020). Both datasets were collected using instruments housed in the Swiss aerosol container on the D-deck of the research vessel Polarstern. Blowing snow events in the observational record were defined based on concurrent 10-m wind speed surpassing a temperature-dependent critical threshold, calculated empirically from the observed air temperature (Li and Pomeroy, 1997), and snowdrift density at 0.1 m above the snow surface, which was required to exceed 10^{-5} kg m^{-3} . These criteria allow separation of snow-driven aerosol production from sea-spray contributions.

We also used observations of sea salt mass from ground stations at three Arctic locations: Villum, Zeppelin, and Alert (Norwegian Institute for Air Research, 2024). Both Alert and Villum are situated above 80°N, where sea ice persists even during summer, making them ideal coastal sites for studying blowing snow events. In contrast, Zeppelin is a mountainous site that is often influenced by sea spray.

2.3 Blowing snow

We implement the same sea-salt aerosol (SSA) production from blowing snow parameterization as used in the TOMCAT chemical transport model in Yang et al. (2019). The parameterization depends on meteorological variables, including air temperature, 10 m wind speed, and relative humidity. The parameterization produces a size-resolved SSA particle flux. The size distribution of emitted SSA follows the original TOMCAT implementation and is determined by the prescribed blowing-snow particle size distribution, snow salinity (which is fixed per size bin), and the assumed number of SSA particles produced per sublimating snow particle. The blowing snow parameterization is most sensitive to how the size distribution is described. Among the input meteorological variables, the blowing-snow parameterization is most sensitive to changes in relative humidity (Ranjithkumar et al., 2025).

https://doi.org/10.5194/egusphere-2026-1575
Preprint. Discussion started: 1 April 2026

2.4 Models

2.4.1 TM5

We employed the Tracer Model version 5 (TM5), a global three-dimensional chemistry transport model designed to simulate atmospheric composition with a focus on tropospheric chemistry (Huijnen et al., 2010). TM5 utilizes a flexible two-way nested zooming capability, allowing for variable horizontal resolutions in different regions of interest. The model incorporates a comprehensive photochemical mechanism, interactions with aerosols, stratospheric chemistry treatments, and both wet and dry deposition processes. Emissions from various sources, including anthropogenic, biogenic, and biomass burning, are integrated with spatial and temporal distributions. Meteorological input fields are typically provided by the ECMWF Integrated Forecasting System (IFS), ensuring realistic transport and mixing processes (Huijnen et al., 2010; Krol et al., 2005; Williams et al., 2017).

For aerosol microphysics, TM5 is coupled with the M7 module, a size-resolved aerosol microphysics scheme that represents the aerosol size distribution using seven log-normal modes (Vignati et al., 2004). These modes include nucleation, Aitken, accumulation, and coarse modes, each further divided into soluble and insoluble fractions. M7 simulates key aerosol processes such as nucleation, condensation, coagulation, and deposition. The module tracks both number and mass concentrations for each mode, allowing a detailed representation of the aerosol dynamics and their interactions with trace gases.

2.4.2 EC-Earth3

For assessing the climate impacts of blowing snow SSA production, we use the EC-Earth3 global climate model (Döscher et al., 2022). In the EC-Earth3 model, aerosols and chemical processes are represented by the TM5 atmospheric chemistry model. The atmospheric model employed a spatial discretization TL255 in the horizontal with 91 vertical levels, whereas TM5 was run at a coarser resolution of 3°×2° (longitude × latitude) with 34 vertical levels and a model top at 0.1 hPa (van Noije et al., 2014).

2.5 Experiments

We conducted six experiments in total, two with the TM5 model and four with EC-Earth3. The TM5 experiments were driven with boundary conditions from ERA5 for the years 2019–2020, corresponding to the MOSAiC campaign period. The EC-Earth3 experiments either followed the AMIP (Gates, 1992) setup described in Naakka et al. (2025), with prescribed sea-ice concentrations and sea surface temperatures taken from the CMIP6 ACCESS-ESM1-5 model for the years 1950–1969, or were carried out in a transient mode following the SSP3-7.0 scenario for years 2015-2051. In all cases, we performed a baseline simulation without the blowing snow parameterization and a sensitivity simulation including sea-salt aerosol (SSA) production from blowing snow. The experiments are listed in table 1.

https://doi.org/10.5194/egusphere-2026-1575
Preprint. Discussion started: 1 April 2026

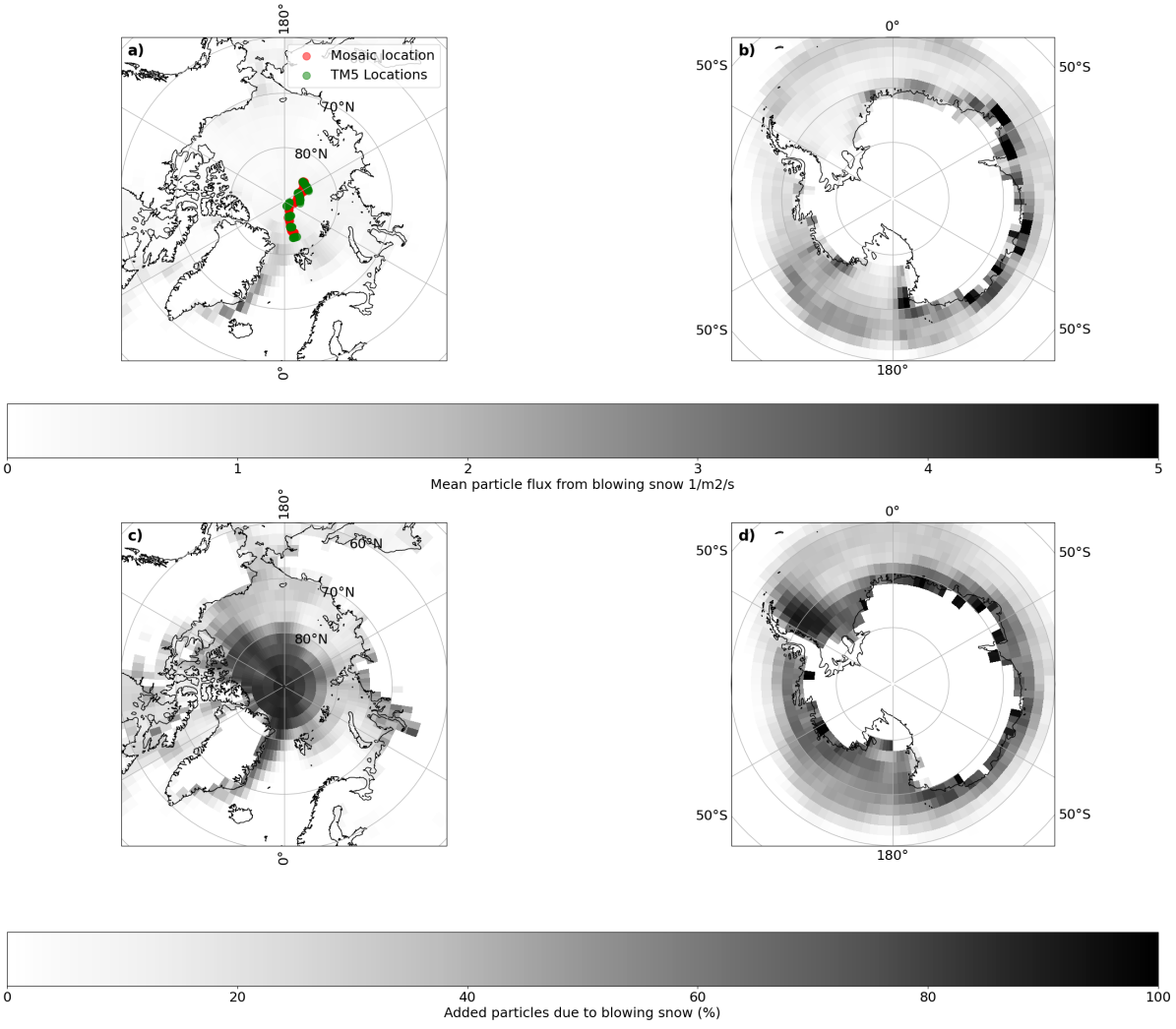

Figure 1. (a) MOSAiC track (red dots) alongside the closest corresponding TM5 model grid point (green dot). The background shading (white to black) indicates the mean sea salt aerosol particle flux from blowing snow events as simulated by the TM5 model. Panel b shows mean sea salt aerosol particle flux from blowing snow for Antarctic regions. Panels c and d show added particles in percent compared to the baseline simulation for Arctic and Antarctic regions.

https://doi.org/10.5194/egusphere-2026-1575
Preprint. Discussion started: 1 April 2026

Table 1. List of experiments used in this study. Each row corresponds to one experiment, with the model name and a brief description.

Experiment Name	Model	Description
Baseline	TM5	2019–2020 with meteorology from ERA5, without blowing snow parametrization
Blowing snow	TM5	2019–2020 with meteorology from ERA5, with blowing snow parametrization
Baseline AMIP	EC-Earth3	AMIP-style run with fixed SST and sea ice, 20-year simulation, without blowing snow parametrization
Blowing snow AMIP	EC-Earth3	AMIP-style run with fixed SST and sea ice, 20-year simulation, with blowing snow parametrization
Baseline transient	EC-Earth3	From 2015-2051 forced by emissions from the SSP3-7.0 scenario, without blowing snow parametrization
Blowing snow transient	EC-Earth3	From 2015-2051 forced by emissions from the SSP3-7.0 scenario, with blowing snow parametrization

3 Comparison with observations

Figure 1 shows the time-mean sea salt particle flux from the TM5 blowing snow experiment. The highest fluxes in the Arctic are found along the eastern coast of Greenland and at the boundary between the open ocean and sea ice. In comparison, the Antarctic exhibits even more pronounced sea salt fluxes from blowing snow. In the Antarctic, emissions are more zonally uniform around the ice edge, whereas in the Arctic they are more localized, particularly near the Greenland coast. Maximum flux values in the Arctic region reach approximately 3.6 particles $m^{-2}\,s^{-1}$, while values in the Antarctic can reach up to 7.0 particles $m^{-2}\,s^{-1}$. This corresponds to an increase in particle number fluxes of over 100% in the Arctic (near the North Pole) and up to 89% in the Antarctic. The high relative increase in the Arctic is due to the lack of other emission sources over sea ice regions. There is a clear seasonal cycle. In the Arctic, most of the sea salt emissions due to blowing snow occur during Boreal wintertime, whereas in the Antarctic the peak emissions occur during the Austral winter (JJA) and spring (SON) seasons (see Fig. S6-S7).

3.1 Comparison to MOSAiC observations

Figure 2 presents a time series of sea salt aerosol number concentrations (particles cm^{-3}) from MOSAiC campaign observations, alongside TM5 model simulations with and without the blowing snow parametrization. The figure demonstrates that inclusion of the blowing snow parametrization in TM5 slightly improves the model's ability to reproduce observed events. The correlation between observation and TM5 baseline is 0.37, while with blowing snow it is 0.39; however the difference between the correlations is not statistically significant using Williams' test. Nevertheless, the model with blowing snow captures a greater number of the observed sea salt aerosol peaks, although some events are still underestimated or missed entirely. In

https://doi.org/10.5194/egusphere-2026-1575
Preprint. Discussion started: 1 April 2026

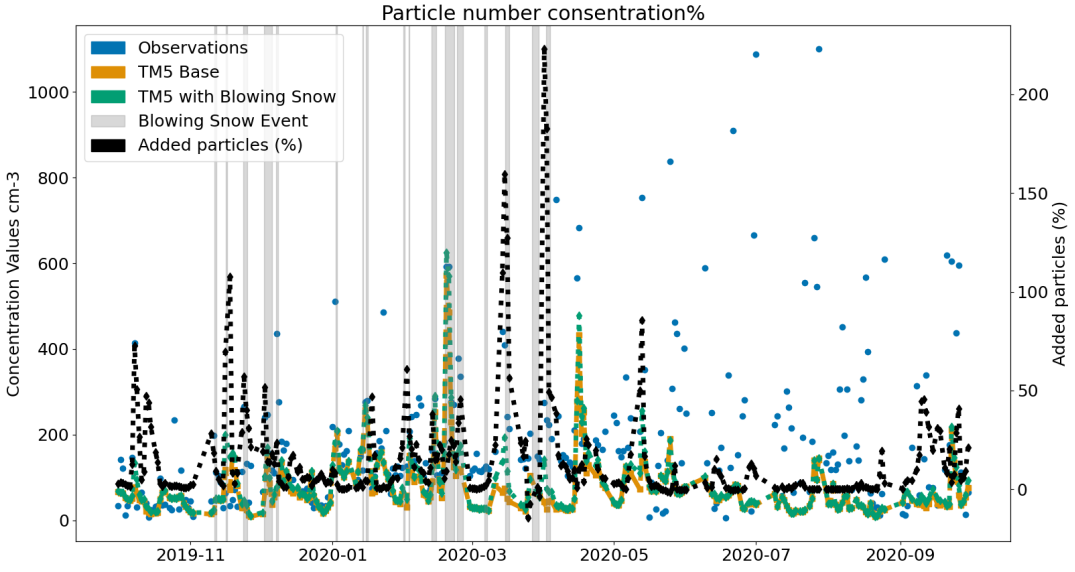

Figure 2. Time series of sea salt aerosol number concentration. The blue line shows observations from the MOSAiC campaign, the orange line represents TM5 model results without blowing snow emissions, and the green line shows TM5 model results including blowing snow emissions. The grey shaded areas indicate periods identified as blowing snow events. The black line represents the estimated number of particles added due to blowing snow emissions in the TM5 simulation.

contrast, the standard model run (without blowing snow) fails to reproduce most of these episodes, highlighting the significance of the blowing snow mechanism for Arctic wintertime aerosol concentrations. The same goes with CCN (see Fig 3). The blowing snow parametrization captures slightly better the CCN increase in blowing snow events, even though not all events are captured.

Figure 4 shows monthly median particle size distributions from TM5 simulations compared to MOSAiC observations and GEOS-Chem model results from Gong et al. (2023). The distributions are plotted as number concentrations ($dN/dlogD_p$) as a function of particle diameter, with each subplot representing a different month. Both TM5 and GEOS-Chem are shown with and without the blowing snow parametrization, allowing for a direct comparison of its impact. The inclusion of blowing snow parametrization leads to an increase in accumulation mode particle concentrations across all months in both models. In March and April, TM5 also exhibits a slight increase in Aitken mode particles when blowing snow is included. In GEOS-Chem, Aitken mode particles increase substantially in all months due to blowing snow.

https://doi.org/10.5194/egusphere-2026-1575
Preprint. Discussion started: 1 April 2026

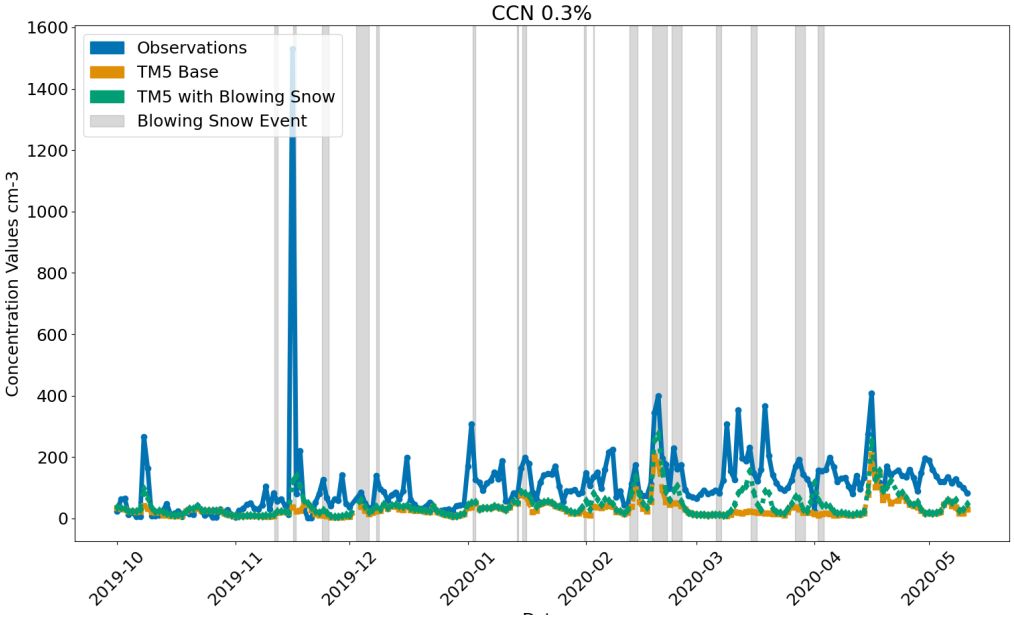

Figure 3. Time series of sea salt CCN concentration. The blue line shows observations from the MOSAiC campaign, the orange line represents TM5 model results without blowing snow emissions, and the green line shows TM5 model results including blowing snow emissions. The grey shaded areas indicate periods identified as blowing snow events.

3.2 Station comparisons

Figure 5 presents monthly sea salt aerosol mass concentrations from TM5 simulations with and without the blowing snow parametrization, alongside observations from three Arctic ground-based monitoring stations: Zeppelin, Alert, and Villum. Across all sites, the inclusion of the blowing snow parametrization leads to a pronounced increase in sea salt concentrations during the winter and spring months (January–May), resulting in a more realistic seasonal cycle. Without blowing snow, TM5 underestimates observed sea salt aerosol levels during the cold season, particularly from January through March. However, the addition of blowing snow leads to an overestimation of the sea salt mass in Villum and Zeppelin.

4 Global effects

4.1 Present-day forcing

The previous section demonstrated how the inclusion of the blowing snow parametrization increases sea salt aerosol mass, particle number concentrations, and CCN locally, particularly in Arctic surface observations. In this section, we assess the global implications of this additional source. Specifically, we examine the effect of blowing snow on global CCN distributions

https://doi.org/10.5194/egusphere-2026-1575
Preprint. Discussion started: 1 April 2026

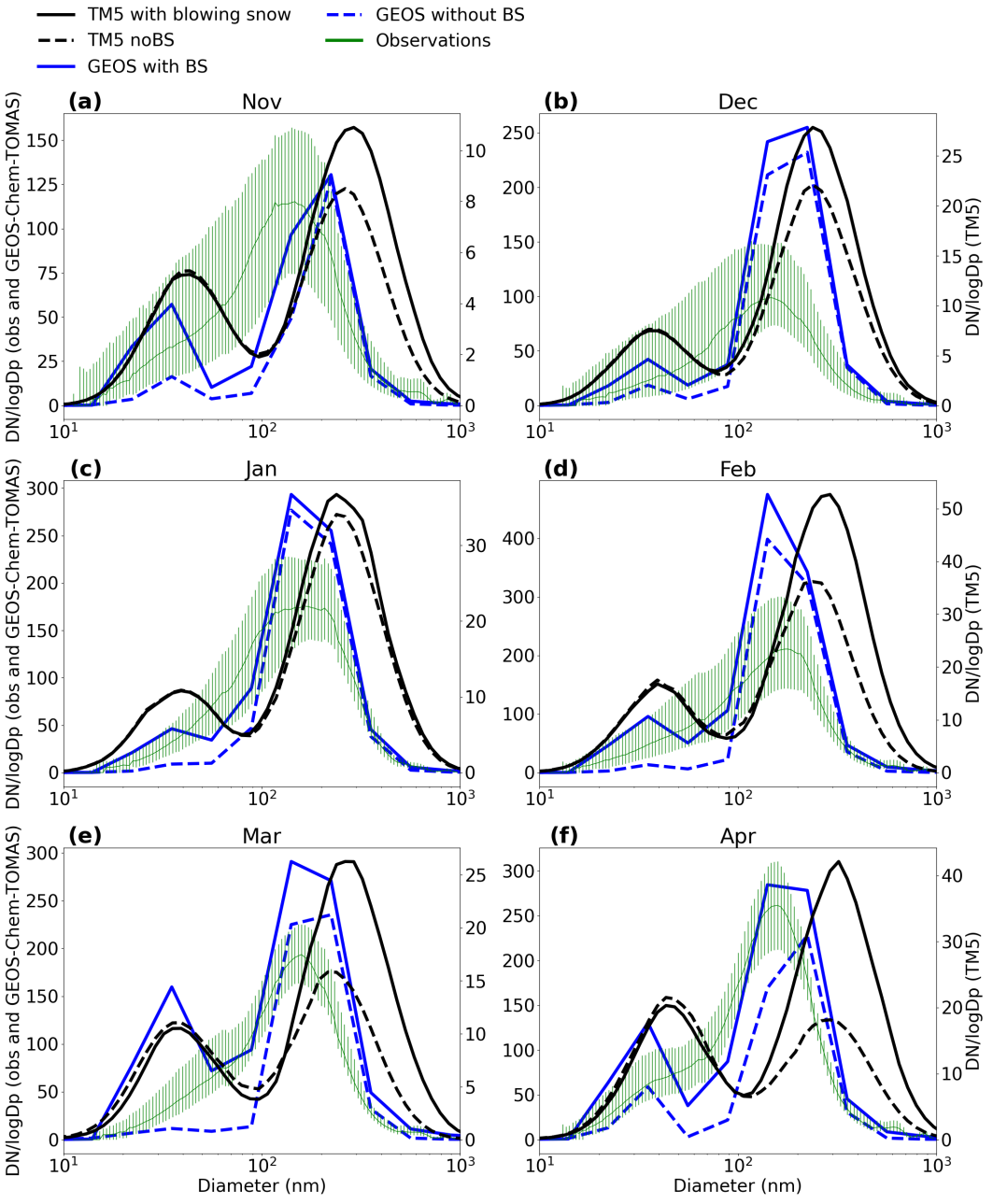

Figure 4. Monthly mean aerosol size distributions along the MOSAiC track. Observations are shown in green. TM5 model results without blowing snow (baseline) are shown as a dashed black line, while TM5 results including blowing snow are shown as a solid black line. GEOS model results without blowing snow are shown as a dashed blue line, and GEOS results with blowing snow are shown as a solid blue line

https://doi.org/10.5194/egusphere-2026-1575
Preprint. Discussion started: 1 April 2026

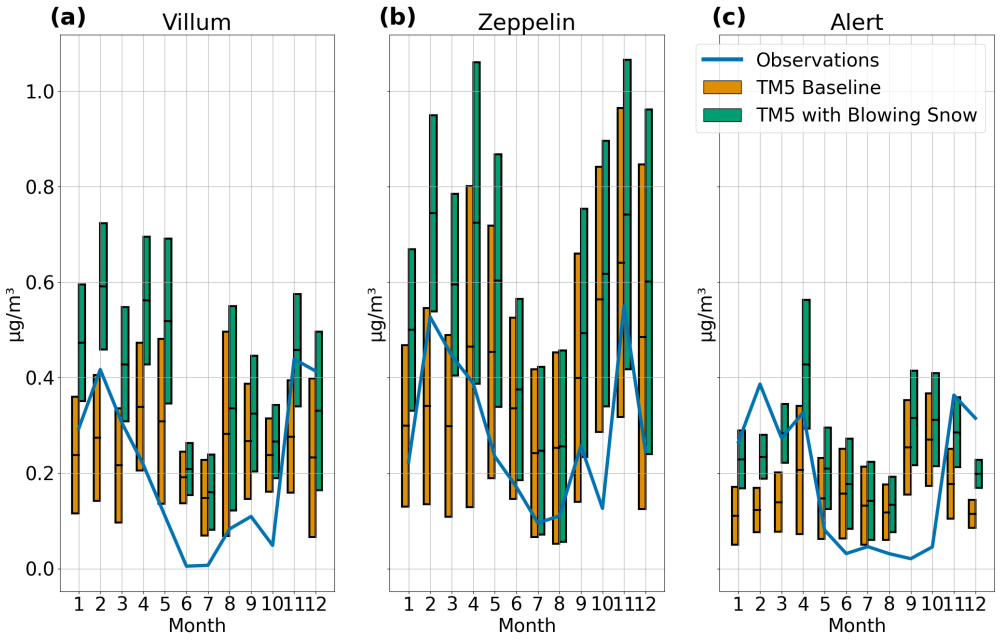

Figure 5. Monthly mean sea salt aerosol mass concentrations at three Arctic land-based stations: Villum, Zeppelin, and Alert. Blue lines represent observations, orange bars show TM5 model results without blowing snow emissions, and green bars show TM5 results including blowing snow emissions. Monthly mean value is indicated by black line, and the height of the bar indicates the standard deviation within the month of modeled sea salt mass.

and quantify the associated radiative forcing. As shown in Figure 1, the strongest impacts are found in the Antarctic region, where extensive sea ice and persistent strong winds create favorable conditions for blowing snow generation.

Figure 6 presents the zonal mean response of aerosol number concentrations to the blowing snow parametrization, with separate panels for the Aitken mode (left) and the accumulation mode (right) particles. The results illustrate that blowing snow significantly increases the number of accumulation mode particles in both the Arctic and Antarctic regions, particularly between 60–80° latitude. This enhancement is most pronounced in the Southern Hemisphere, consistent with the stronger sea salt fluxes over Antarctic sea ice.

In contrast, the inclusion of blowing snow leads to a widespread reduction in Aitken mode particle concentrations across the same regions. This suggests that the added coarse and accumulation mode sea salt particles enhance coagulation and act as a sink for ultrafine particles, reducing their atmospheric lifetime. However, in Figure 4 the GEOS model also shows an increase of Aitken mode particles, in comparison to TM5 which shows a slight decrease of Aitken mode particles. The opposing responses in the two size modes highlight the complex role of blowing snow in modulating the aerosol size distribution and its potential implications for cloud condensation nuclei (CCN) availability and cloud microphysical properties in polar environments.

https://doi.org/10.5194/egusphere-2026-1575
Preprint. Discussion started: 1 April 2026

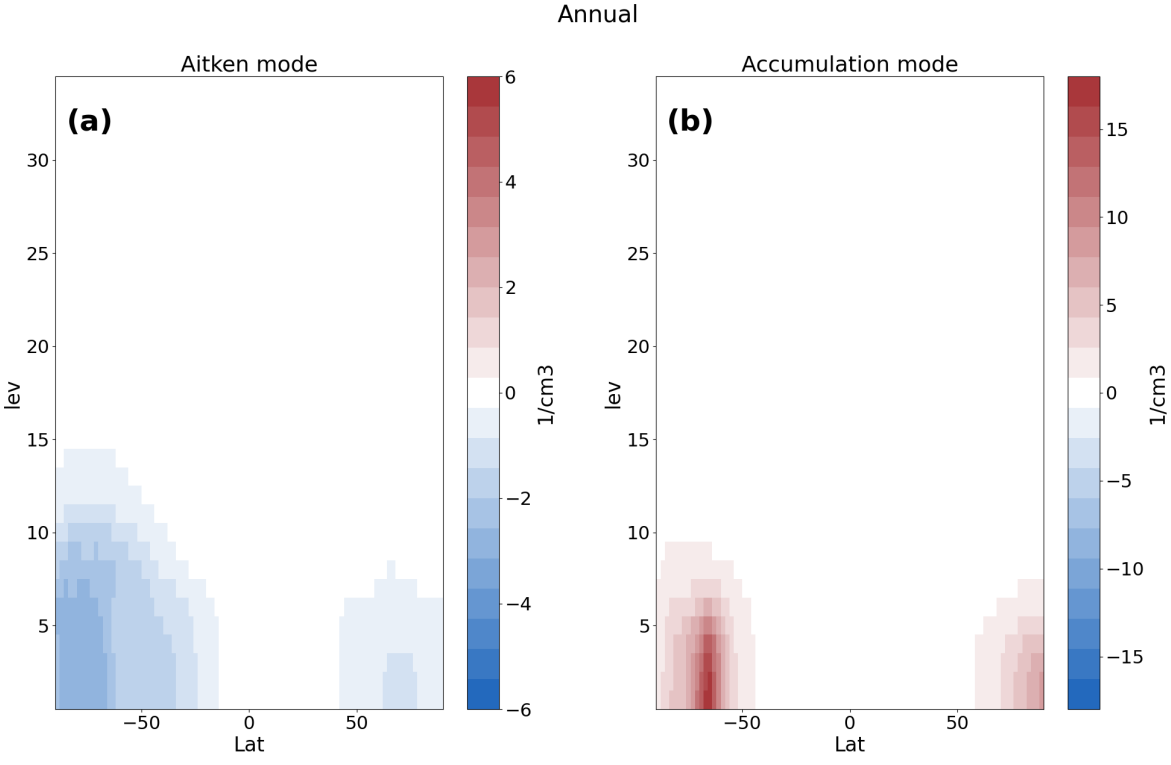

Figure 6. Annual zonal mean difference in particle number concentration due to blowing snow for the Aitken mode (left) and accumulation mode (right) in the TM5 simulations. Shading shows the change in number concentration (particles cm^{-3}), calculated as the difference between simulations with and without blowing snow emissions. Positive values indicate an increase in concentration attributed to blowing snow events. All colored region are statistically significant at level $p < 0.05$

https://doi.org/10.5194/egusphere-2026-1575
Preprint. Discussion started: 1 April 2026

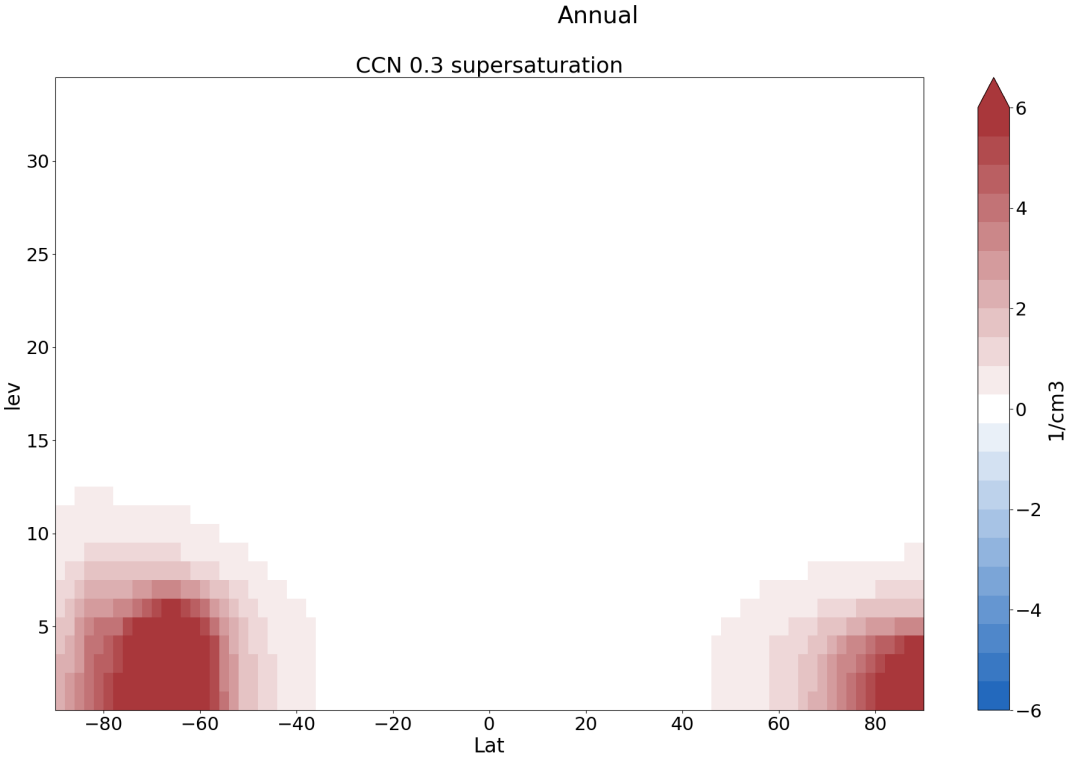

Figure 7. Annual zonal mean difference in CCN concentration in the TM5 simulations. All colored region are statistically significant at level $p < 0.05$.

Figure 7 shows the zonal mean change in CCN concentrations at 0.3% supersaturation due to the inclusion of the blowing snow parametrization. The results highlight a clear polar enhancement, with the strongest increases observed in the Antarctic. Specifically, CCN concentrations increase by up to 16.85 cm^{-3} in the Antarctic and 8.31 cm^{-3} in the Arctic. These increases are consistent with the elevated sea salt aerosol concentrations resulting from blowing snow emissions in both hemispheres. The enhancement in CCN is primarily confined to latitudes poleward of 60°.

The inclusion of the blowing-snow parametrization in EC-Earth leads to statistically significant changes in several surface radiative flux components (Fig. 8). In Arctic sea-ice-covered regions, enhanced production of SSA from blowing snow results in a marked increase in the net downward surface radiative flux, mainly due to increased downward longwave radiation. The additional SSA increases CCN, thereby strengthening the longwave cloud radiative effect. This mechanism explains why the largest changes occur in winter, when blowing-snow events are most frequent (Fig. S3).

https://doi.org/10.5194/egusphere-2026-1575
Preprint. Discussion started: 1 April 2026

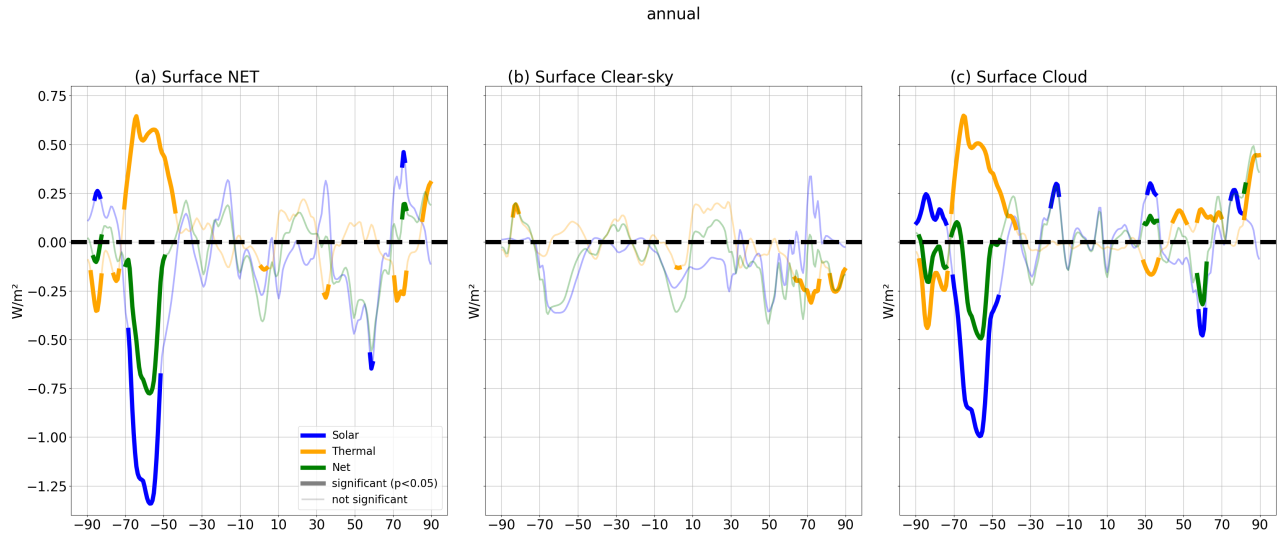

Figure 8. Zonal mean annual-mean changes in surface radiative fluxes (W m^{-2}) simulated with EC-Earth3, comparing AMIP-type experiments with and without the blowing snow sea-salt aerosol parameterization. Left: all-sky surface radiative fluxes, middle: clear-sky contributions, right: cloud radiative effects. Shown are changes in new downward solar (blue), thermal (orange), and net (green) components.

A notable decrease in longwave clear-sky flux is also found over the Arctic Ocean, indicating a drier lower troposphere in the blowing-snow experiment. The opposite signs of the cloud and clear-sky components during winter suggest that the enhanced CCN supply modifies both cloud microphysics and the thermodynamical structure of the near-surface atmosphere. Spatially, the annual-mean surface radiative forcing exhibits distinct regional patterns (Fig. S1): shortwave changes are strongest over high-latitude land areas, whereas longwave changes dominate over perennial sea-ice regions. This separation reflects differences in surface albedo, cloud response, and the vertical distribution of the added SSA.

In the Southern Ocean around Antarctica, the downward LW flux is increased significantly in the blowing snow experiment due to increased cloud longwave radiative effect at the surface. However, as a difference to the Arctic region, the increased longwave radiation is more than compensated by reduced shortwave radiation. This results primarily from a stronger negative cloud shortwave effect but also from reduced clear-sky shortwave radiation, which is likely due to the sea-salt direct radiative effect. Consequently, in the Southern Ocean, the net downward radiation at the surface is more negative in the blowing snow experiment. Seasonally, this difference in most pronounced in the Austral summer (DJF) (Figs. S4 and S5).

Overall, the results show that blowing-snow-derived SSA exerts a seasonally and regionally dependent radiative influence, with wintertime cloud modifications playing the primary role in increasing the net downward surface energy flux in the Arctic, and summertime cloud modifications decreasing it around the Antarctica.

https://doi.org/10.5194/egusphere-2026-1575
Preprint. Discussion started: 1 April 2026

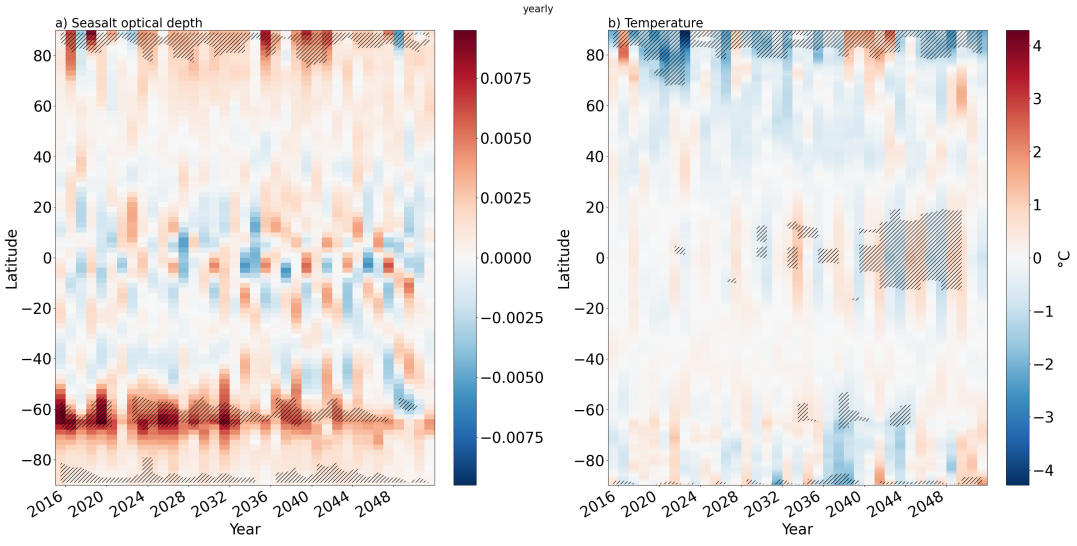

Figure 9. Zonal-mean time evolution of (a) sea-salt aerosol optical depth (AOD) and (b) surface air temperature differences between transient EC-Earth3 simulations with and without the blowing-snow parameterization, driven by SSP3–7.0 emissions. Shaded areas indicate regions where differences are statistically significant at $p < 0.05$ after false discovery rate (FDR) correction.

4.2 Future response under SSP370 with interactive SST

Figure 9a presents the evolution of sea-salt AOD. The largest increases occur over the Southern Ocean, with substantial enhancements also evident in the Arctic, consistent with elevated sea-salt emissions from blowing snow. In the Southern Ocean, the AOD difference tends to decrease slighly towards the end of the simulation period, consistent with the fact that with warming climate, sea ice cover is reduced, which acts to reduce the blowing snow emissions. Figure 9b shows the corresponding evolution of surface air temperature. The most notable feature is that the inclusion of SSA from blowing snow induces some regional cooling in the Arctic, by up to $4°C$ in some years. Even though the Arctic cooling is statistically significant, we suspect that this feature is caused by internal variability. The cooling is surprising, because in the AMIP-type runs, the change in net radiative flux at the surface was slightly positive (Fig. 8a). Furthermore, while most blowing-snow emissions occur over the Southern Ocean, and the net radiative flux response is negative in the AMIP-type runs, only very weak cooling is found there. It is further noted that some statistically significant temperature anomalies appear in the tropics, but their lack of spatial and temporal coherence suggests they arise from internal variability rather than a physically consistent forcing response. Overall, blowing-snow-driven sea-salt production induces regional cooling in both polar regions in EC-Earth3. However, the magnitude, intermittency, and spatial structure of the response indicate that internal climate variability partly masks or modulates the forced signal, particularly outside high latitudes.

https://doi.org/10.5194/egusphere-2026-1575
Preprint. Discussion started: 1 April 2026

5 Discussion

Modeling SSA production from blowing snow is subject to significant uncertainties stemming from observational gaps and intrinsic variability in snow properties and meteorological parameters.The particle size distribution of snow particles is the parameter to which the SSA number flux is most sensitive. Shape and scale parameters defining this distribution strongly control modeled aerosol emissions, yet observational constraints for these parameters remain limited and highly variable. Complicating matters further, parameters such as wind speed, snow age, and atmospheric humidity also introduce mid-level to high sensitivity to the the parametrization of SSA production from blowing snow (Ranjithkumar et al., 2025).

It is not only the parameterization of blowing snow that introduces uncertainties in estimating sea-salt aerosol (SSA) production and its climate impacts. Different models show both similarities and differences in how their aerosol schemes respond to additional SSA production from blowing snow. In particular, the number concentration of accumulation-mode particles is increased in both the TM5 and GEOS models; however, a notable discrepancy is that in TM5, adding blowing-snow SSA decreases Aitken-mode particles, whereas in the GEOS model it increases them. This likely relates to differences in how aerosol modes are represented in the two models.(Swanson et al., 2022; Huang et al., 2020). In TM5, blowing-snow SSA enhances accumulation-mode particles but decreases Aitken-mode particles due to efficient transfer via coagulation and condensation into larger modes, effectively shifting the particle population toward larger sizes (Gliß et al., 2021). In GEOS, by contrast, blowing-snow SSA increases Aitken-mode particles because of a less aggressive transfer into larger modes, reflecting its more detailed representation of the aerosol size distribution.

Perhaps the most interesting finding is that, in EC-Earth3, the Arctic exhibits a cooling response when the blowing-snow sea-salt source is included. This is in contrast to previous studies, which generally report a warming effect. For example, Gong et al. (2023) found that including blowing snow increases the longwave emissivity of clouds, leading to a surface warming of approximately +2.3 $\mathrm{W\,m^{-2}}$ under cloudy-sky conditions. Similarly, Ji et al. (2025) showed that wet growth of sea-salt aerosols under high relative humidity intensifies surface warming.

6 Conclusions

This study investigates how sea salt aerosols (SSA) generated from blowing snow influence cloud properties and the surface radiation budget. We implemented a parameterization of SSA production from blowing snow in the TM5 global chemical transport model and the EC-Earth3 global climate model. Our analysis focuses on the resulting changes in aerosol particle mass, cloud condensation nuclei (CCN) concentrations, and the surface radiation budget.

First, we find that SSA production from blowing snow events is more stronger in Antarctic than in Arctic regions. In TM5, blowing snow increases particle number concentrations in the 100–1000 nm size range, while the GEOS model shows an increase in smaller particle numbers as well. With blowing snow included, TM5 better captures observed peaks in SSA particle number concentrations. In coastal regions, blowing snow enhances the seasonal cycle, with higher particle concentrations during winter and spring.

https://doi.org/10.5194/egusphere-2026-1575
Preprint. Discussion started: 1 April 2026

The inclusion of SSA from blowing snow leads to increased CCN concentrations. Globally, blowing snow generates a negative radiative forcing at the surface due to reduced incoming solar radiation, while modifications to cloud properties contribute to a positive change in the longwave (LW) radiation balance.

Code availability. Code used to generate plots are available https://github.com/kallenordling/blowing_from_snow/

Data availability. All simulation data is available at https://doi.org/10.5281/zenodo.19327654, Station observatiosn can be downloaded from https://ebas.nilu.no/ and Mosaic is from https://www.pangaea.de/?q=project:label:MOSAiC

Author contributions. KN and PR did the simulation, JM and RM came up with original idea. Kn wrote initial draft where all authors commented

Competing interests. no competing interests are present

Acknowledgements. We also acknowledge the Academy of Finland (grant no. 337552)

https://doi.org/10.5194/egusphere-2026-1575
Preprint. Discussion started: 1 April 2026

References

Acosta Navarro, J. C., Varma, V., Riipinen, I., Seland, Ø., Kirkevåg, A., Struthers, H., Iversen, T., Hansson, H.-C., and Ekman, A. M. L.: Amplification of Arctic warming by past air pollution reductions in Europe, Nature Geoscience, 9, 277–281, https://doi.org/10.1038/ngeo2673, 2016.

Beck, I., Quéléver, L., Laurila, T., Jokinen, T., and Schmale, J.: Continuous corrected particle number concentration data in 10 sec resolution, measured in the Swiss aerosol container during MOSAiC 2019/2020, https://doi.org/10.1594/PANGAEA.941886, 2022.

Bergner, N., Heutte, B., Angot, H., Dada, L., Beck, I., Quéléver, L., Jokinen, T., Laurila, T., and Schmale, J.: Cloud Condensation Nuclei (CCN) concentrations at 0.3% supersaturation level measured in the Swiss container during MOSAiC 2019/2020, PANGAEA, https://doi.org/10.1594/PANGAEA.961135, in: Bergner, N et al. (2023): Cloud Condensation Nuclei (CCN) concentrations measured in the Swiss container during MOSAiC 2019/2020 [dataset publication series]. PANGAEA, https://doi.org/10.1594/PANGAEA.961131, 2023.

Döscher, R., Acosta, M., Alessandri, A., Anthoni, P., Arsouze, T., Bergman, T., Bernardello, R., Boussetta, S., Caron, L.-P., Carver, G., Castrillo, M., Catalano, F., Cvijanovic, I., Davini, P., Dekker, E., Doblas-Reyes, F. J., Docquier, D., Echevarria, P., Fladrich, U., Fuentes-Franco, R., Gröger, M., v. Hardenberg, J., Hieronymus, J., Karami, M. P., Keskinen, J.-P., Koenigk, T., Makkonen, R., Massonnet, F., Ménégoz, M., Miller, P. A., Moreno-Chamarro, E., Nieradzik, L., van Noije, T., Nolan, P., O'Donnell, D., Ollinaho, P., van den Oord, G., Ortega, P., Prims, O. T., Ramos, A., Reerink, T., Rousset, C., Ruprich-Robert, Y., Le Sager, P., Schmith, T., Schrödner, R., Serva, F., Sicardi, V., Sloth Madsen, M., Smith, B., Tian, T., Tourigny, E., Uotila, P., Vancoppenolle, M., Wang, S., Wårlind, D., Willén, U., Wyser, K., Yang, S., Yepes-Arbós, X., and Zhang, Q.: The EC-Earth3 Earth system model for the Coupled Model Intercomparison Project 6, Geoscientific Model Development, 15, 2973–3020, https://doi.org/10.5194/gmd-15-2973-2022, 2022.

Emme, E. J. and Horowitz, H. M.: Impacts of sea ice leads on sea salt aerosols and atmospheric chemistry in the Arctic, Atmospheric Chemistry and Physics, 25, 4531–4545, https://doi.org/10.5194/acp-25-4531-2025, 2025.

Frey, M. M., Norris, S. J., Brooks, I. M., Anderson, P. S., Nishimura, K., Yang, X., Jones, A. E., Nerentorp Mastromonaco, M. G., Jones, D. H., and Wolff, E. W.: First direct observation of sea salt aerosol production from blowing snow above sea ice, Atmospheric Chemistry and Physics, 20, 2549–2578, https://doi.org/10.5194/acp-20-2549-2020, 2020.

Gates, W. L.: AN AMS CONTINUING SERIES: GLOBAL CHANGE–AMIP: The Atmospheric Model Intercomparison Project, Bulletin of the American Meteorological Society, 73, 1962 – 1970, https://doi.org/10.1175/1520-0477(1992)073<1962:ATAMIP>2.0.CO;2, 1992.

Gliß, J., Mortier, A., Schulz, M., Andrews, E., Balkanski, Y., Bauer, S. E., Benedictow, A. M. K., Bian, H., Checa-Garcia, R., Chin, M., Ginoux, P., Griesfeller, J. J., Heckel, A., Kipling, Z., Kirkevåg, A., Kokkola, H., Laj, P., Le Sager, P., Lund, M. T., Lund Myhre, C., Matsui, H., Myhre, G., Neubauer, D., van Noije, T., North, P., Olivié, D. J. L., Rémy, S., Sogacheva, L., Takemura, T., Tsigaridis, K., and Tsyro, S. G.: AeroCom phase III multi-model evaluation of the aerosol life cycle and optical properties using ground- and space-based remote sensing as well as surface in situ observations, Atmospheric Chemistry and Physics, 21, 87–128, https://doi.org/10.5194/acp-21-87-2021, 2021.

Gong, X., Zhang, J., Croft, B., Yang, X., Frey, M. M., Bergner, N., Chang, R. Y.-W., Creamean, J. M., Kuang, C., Martin, R. V., Ranjithkumar, A., Sedlacek, A. J., Uin, J., Willmes, S., Zawadowicz, M. A., Pierce, J. R., Shupe, M. D., Schmale, J., and Wang, J.: Arctic warming by abundant fine sea salt aerosols from blowing snow, Nature Geoscience, 16, 768–774, https://doi.org/10.1038/s41561-023-01254-8, 2023.

Huang, J., Jaeglé, L., and Shah, V.: Using CALIOP to constrain blowing snow emissions of sea salt aerosols over Arctic and Antarctic sea ice, Atmospheric Chemistry and Physics, 18, 16 253–16 269, https://doi.org/10.5194/acp-18-16253-2018, 2018.

https://doi.org/10.5194/egusphere-2026-1575
Preprint. Discussion started: 1 April 2026

Huang, J., Jaeglé, L., Chen, Q., Alexander, B., Sherwen, T., Evans, M. J., Theys, N., and Choi, S.: Evaluating the impact of blowing-snow sea salt aerosol on springtime BrO and O_3 in the Arctic, Atmospheric Chemistry and Physics, 20, 7335–7358, https://doi.org/10.5194/acp-20-7335-2020, 2020.

Huijnen, V., Williams, J., van Weele, M., van Noije, T., Krol, M., Dentener, F., Segers, A., Houweling, S., Peters, W., de Laat, J., Boersma, F., Bergamaschi, P., van Velthoven, P., Le Sager, P., Eskes, H., Alkemade, F., Scheele, R., Nédélec, P., and Pätz, H.-W.: The global chemistry transport model TM5: description and evaluation of the tropospheric chemistry version 3.0, Geoscientific Model Development, 3, 445–473, https://doi.org/10.5194/gmd-3-445-2010, 2010.

Ji, D., Palm, M., Buschmann, M., Ebell, K., Maturilli, M., Sun, X., and Notholt, J.: Hygroscopic aerosols amplify longwave downward radiation in the Arctic, Atmospheric Chemistry and Physics, 25, 3889–3904, https://doi.org/10.5194/acp-25-3889-2025, 2025.

Krol, M., Houweling, S., Bregman, B., van den Broek, M., Segers, A., van Velthoven, P., Peters, W., Dentener, F., and Bergamaschi, P.: The two-way nested global chemistry-transport zoom model TM5: algorithm and applications, Atmospheric Chemistry and Physics, 5, 417–432, https://doi.org/10.5194/acp-5-417-2005, 2005.

Lapere, R., Thomas, J. L., Marelle, L., Ekman, A. M. L., Frey, M. M., Lund, M. T., Makkonen, R., Ranjithkumar, A., Salter, M. E., Samset, B. H., Schulz, M., Sogacheva, L., Yang, X., and Zieger, P.: The Representation of Sea Salt Aerosols and Their Role in Polar Climate Within CMIP6, Journal of Geophysical Research: Atmospheres, 128, e2022JD038 235, https://doi.org/https://doi.org/10.1029/2022JD038235, e2022JD038235 2022JD038235, 2023.

Lapere, R., Marelle, L., Rampal, P., Brodeau, L., Melsheimer, C., Spreen, G., and Thomas, J. L.: Modeling the contribution of leads to sea spray aerosol in the high Arctic, Atmospheric Chemistry and Physics, 24, 12 107–12 132, https://doi.org/10.5194/acp-24-12107-2024, 2024.

Lewinschal, A., Ekman, A. M. L., Hansson, H.-C., Sand, M., Berntsen, T. K., and Langner, J.: Local and remote temperature response of regional SO_2 emissions, Atmospheric Chemistry and Physics, 19, 2385–2403, https://doi.org/10.5194/acp-19-2385-2019, 2019.

Li, L. and Pomeroy, J. W.: Probability of occurrence of blowing snow, Journal of Geophysical Research: Atmospheres, 102, 21 955–21 964, https://doi.org/https://doi.org/10.1029/97JD01522, 1997.

Mauritsen, T., Sedlar, J., Tjernström, M., Leck, C., Martin, M., Shupe, M., Sjogren, S., Sierau, B., Persson, P. O. G., Brooks, I. M., and Swietlicki, E.: An Arctic CCN-limited cloud-aerosol regime, Atmospheric Chemistry and Physics, 11, 165–173, https://doi.org/10.5194/acp-11-165-2011, 2011.

May, N. W., Quinn, P. K., McNamara, S. M., and Pratt, K. A.: Multiyear study of the dependence of sea salt aerosol on wind speed and sea ice conditions in the coastal Arctic, Journal of Geophysical Research: Atmospheres, 121, 9208–9219, https://doi.org/https://doi.org/10.1002/2016JD025273, 2016.

Merikanto, J., Nordling, K., Räisänen, P., Räisänen, J., O'Donnell, D., Partanen, A.-I., and Korhonen, H.: How Asian aerosols impact regional surface temperatures across the globe, Atmospheric Chemistry and Physics, 21, 5865–5881, https://doi.org/10.5194/acp-21-5865-2021, 2021.

Naakka, T., Köhler, D., Nordling, K., Räisänen, P., Lund, M. T., Makkonen, R., Merikanto, J., Samset, B. H., Sinclair, V. A., Thomas, J. L., and Ekman, A. M. L.: Polar winter climate change: strong local effects from sea ice loss, widespread consequences from warming seas, Atmospheric Chemistry and Physics, 25, 8127–8145, https://doi.org/10.5194/acp-25-8127-2025, 2025.

Norwegian Institute for Air Research: EBAS Database, https://ebas.nilu.no/, data set, last access: 21 Feb 2025, 2024.

Pithan, F. and Mauritsen, T.: Arctic amplification dominated by temperature feedbacks in contemporary climate models, Nature Geoscience, 7, 181–184, https://doi.org/10.1038/ngeo2071, 2014.

https://doi.org/10.5194/egusphere-2026-1575
Preprint. Discussion started: 1 April 2026

Ranjithkumar, A., Duncan, E., Yang, X., Partridge, D. G., Lachlan-Cope, T., Gong, X., Nishimura, K., and Frey, M. M.: Direct observation of Arctic Sea salt aerosol production from blowing snow and modeling over a changing sea ice environment, Elementa: Science of the Anthropocene, 13, 00 006, https://doi.org/10.1525/elementa.2024.00006, 2025.

Rantanen, M., Karpechko, A. Y., Lipponen, A., Nordling, K., Hyvärinen, O., Ruosteenoja, K., Vihma, T., and Laaksonen, A.: The Arctic has warmed nearly four times faster than the globe since 1979, Communications Earth & Environment, 3, 168, https://doi.org/10.1038/s43247-022-00498-3, 2022.

Sand, M., Samset, B. H., Balkanski, Y., Bauer, S., Bellouin, N., Berntsen, T. K., Bian, H., Chin, M., Diehl, T., Easter, R., Ghan, S. J., Iversen, T., Kirkevåg, A., Lamarque, J.-F., Lin, G., Liu, X., Luo, G., Myhre, G., Noije, T. V., Penner, J. E., Schulz, M., Seland, Ø., Skeie, R. B., Stier, P., Takemura, T., Tsigaridis, K., Yu, F., Zhang, K., and Zhang, H.: Aerosols at the poles: an AeroCom Phase II multi-model evaluation, Atmospheric Chemistry and Physics, 17, 12 197–12 218, https://doi.org/10.5194/acp-17-12197-2017, 2017.

Schmale, J., Zieger, P., and Ekman, A. M. L.: Aerosols in current and future Arctic climate, Nature Climate Change, 11, 95–105, https://doi.org/10.1038/s41558-020-00969-5, 2021.

Serreze, M. C. and Barry, R. G.: Processes and impacts of Arctic amplification: A research synthesis, Global and Planetary Change, 77, 85–96, https://doi.org/https://doi.org/10.1016/j.gloplacha.2011.03.004, 2011.

Shupe, M. D., Rex, M., Dethloff, K., Damm, E., Fong, A. A., Gradinger, R., Heuzé, C., Loose, B., Makarov, A., Maslowski, W., Nicolaus, M., Perovich, D., Rabe, B., Rinke, A., Sokolov, V., and Sommerfeld, A.: Arctic Report Card 2020: The MOSAiC Expedition: A Year Drifting with the Arctic Sea Ice, Administrative report, United States. National Oceanic and Atmospheric Administration. Office of Oceanic and Atmospheric Research. Physical Sciences Laboratory (U.S.) and Cooperative Institute for Research in the Atmosphere (Fort Collins, Colo.), https://doi.org/10.25923/9g3v-xh92, 2020.

Swanson, W. F., Holmes, C. D., Simpson, W. R., Confer, K., Marelle, L., Thomas, J. L., Jaeglé, L., Alexander, B., Zhai, S., Chen, Q., Wang, X., and Sherwen, T.: Comparison of model and ground observations finds snowpack and blowing snow aerosols both contribute to Arctic tropospheric reactive bromine, Atmospheric Chemistry and Physics, 22, 14 467–14 488, https://doi.org/10.5194/acp-22-14467-2022, 2022.

Thornhill, G., Collins, W., Olivié, D., Skeie, R. B., Archibald, A., Bauer, S., Checa-Garcia, R., Fiedler, S., Folberth, G., Gjermundsen, A., Horowitz, L., Lamarque, J.-F., Michou, M., Mulcahy, J., Nabat, P., Naik, V., O'Connor, F. M., Paulot, F., Schulz, M., Scott, C. E., Séférian, R., Smith, C., Takemura, T., Tilmes, S., Tsigaridis, K., and Weber, J.: Climate-driven chemistry and aerosol feedbacks in CMIP6 Earth system models, Atmospheric Chemistry and Physics, 21, 1105–1126, https://doi.org/10.5194/acp-21-1105-2021, 2021.

van Noije, T. P. C., Le Sager, P., Segers, A. J., van Velthoven, P. F. J., Krol, M. C., Hazeleger, W., Williams, A. G., and Chambers, S. D.: Simulation of tropospheric chemistry and aerosols with the climate model EC-Earth, Geoscientific Model Development, 7, 2435–2475, https://doi.org/10.5194/gmd-7-2435-2014, 2014.

Venugopal, A. U., Bhatti, Y. A., Morgenstern, O., Williams, J., Edkins, N., Hardacre, C., Jones, A., and Revell, L. E.: Constraining the Uncertainty Associated With Sea Salt Aerosol Parameterizations in Global Models Using Nudged UKESM1-AMIP Simulations, Journal of Geophysical Research: Atmospheres, 130, e2024JD041 643, https://doi.org/https://doi.org/10.1029/2024JD041643, e2024JD041643 2024JD041643, 2025.

Vignati, E., Wilson, J., and Stier, P.: M7: An efficient size-resolved aerosol microphysics module for large-scale aerosol transport models, Journal of Geophysical Research: Atmospheres, 109, https://doi.org/https://doi.org/10.1029/2003JD004485, 2004.

Wendisch, M., Macke, A., Ehrlich, A., Lüpkes, C., Mech, M., Chechin, D., Dethloff, K., Velasco, C. B., Bozem, H., Brückner, M., Clemen, H.-C., Crewell, S., Donth, T., Dupuy, R., Ebell, K., Egerer, U., Engelmann, R., Engler, C., Eppers, O., Gehrmann, M., Gong, X., Gottschalk, M., Gourbeyre, C., Griesche, H., Hartmann, J., Hartmann, M., Heinold, B., Herber, A., Herrmann, H., Heygster, G., Hoor, P.,

https://doi.org/10.5194/egusphere-2026-1575
Preprint. Discussion started: 1 April 2026

Jafariserajehlou, S., Jäkel, E., Järvinen, E., Jourdan, O., Kästner, U., Kecorius, S., Knudsen, E. M., Köllner, F., Kretzschmar, J., Lelli, L., Leroy, D., Maturilli, M., Mei, L., Mertes, S., Mioche, G., Neuber, R., Nicolaus, M., Nomokonova, T., Notholt, J., Palm, M., van Pinxteren, M., Quaas, J., Richter, P., Ruiz-Donoso, E., Schäfer, M., Schmieder, K., Schnaiter, M., Schneider, J., Schwarzenböck, A., Seifert, P., Shupe, M. D., Siebert, H., Spreen, G., Stapf, J., Stratmann, F., Vogl, T., Welti, A., Wex, H., Wiedensohler, A., Zanatta, M., and Zeppenfeld, S.: The Arctic Cloud Puzzle: Using ACLOUD/PASCAL Multiplatform Observations to Unravel the Role of Clouds and Aerosol Particles in Arctic Amplification, Bulletin of the American Meteorological Society, 100, 841 – 871, https://doi.org/10.1175/BAMS-D-18-0072.1, 2019.

Williams, J. E., Boersma, K. F., Le Sager, P., and Verstraeten, W. W.: The high-resolution version of TM5-MP for optimized satellite retrievals: description and validation, Geoscientific Model Development, 10, 721–750, https://doi.org/10.5194/gmd-10-721-2017, 2017.

Yang, X., Pyle, J. A., and Cox, R. A.: Sea salt aerosol production and bromine release: Role of snow on sea ice, Geophysical Research Letters, 35, https://doi.org/https://doi.org/10.1029/2008GL034536, 2008.

Yang, X., Frey, M. M., Rhodes, R. H., Norris, S. J., Brooks, I. M., Anderson, P. S., Nishimura, K., Jones, A. E., and Wolff, E. W.: Sea salt aerosol production via sublimating wind-blown saline snow particles over sea ice: parameterizations and relevant microphysical mechanisms, Atmospheric Chemistry and Physics, 19, 8407–8424, https://doi.org/10.5194/acp-19-8407-2019, 2019.